molecular microbiology

Binding of the RNA chaperone Hfq to the type IV pilus base is crucial for its function in *Synechocystis* sp. PCC 6803

Journal:	*Molecular Microbiology*
Manuscript ID:	MMI-2013-13827.R1
Manuscript Type:	Research Article
Date Submitted by the Author:	13-Mar-2014
Complete List of Authors:	Nils, Schuergers; University Freiburg, Institute of Biology IIII Ruppert, Ulrike; Justus-Liebig-University Giessen, Institute of Micro- and Molecular Biology Watanabe, Satoru; Tokyo University of Agriculture, Bioscience Nuernberg, Dennis; Queen Mary University of London, School of Biological and Chemical Sciences Lochnit, Günter; Justus Liebig University, Institute of Biochemistry Dienst, Dennis; Institute of Biology, Plant Biochemistry; Mullineaux, Conrad; Queen Mary University of London, School of Biological and Chemical Sciences Wilde, Annegret; University Freiburg, Institute of Biology III
Key Words:	Hfq, phototaxis, type IV pili, PilB, cyanobacteria

Binding of the RNA chaperone Hfq to the type IV pilus base is crucial for its function in *Synechocystis* sp. PCC 6803

Nils Schuergers[1], Ulrike Ruppert[2], Satoru Watanabe[3], Dennis J. Nuernberg[4], Günter Lochnit[5], Dennis Dienst[6], Conrad W. Mullineaux[4], Annegret Wilde[1,*]

[1]Molekulare Genetik, Fakultät für Biologie, Albert-Ludwigs-Universität Freiburg, D-79104 Freiburg, Germany

[2]Institut für Mikrobiologie und Molekularbiologie, Justus-Liebig-Universität Giessen, D-35392 Giessen, Germany

[3]Department of Bioscience, Tokyo University of Agriculture, Tokyo 156-8502, Japan

[4]School of Biological and Chemical Sciences, Queen Mary University of London, London E1 4NS, UK

[5]Institut für Biochemie, Justus-Liebig-Universität Giessen, D-35392 Giessen, Germany

[6]Institut für Biologie, Humboldt-Universität zu Berlin, D-10115 Berlin, Germany

[*] For Correspondence. E-mail Annegret.Wilde@biologie.uni-freiburg.de; Tel. +49 (0) 76120397828; Fax +49 (0) 761-203-2745

Running Title

Localization of Hfq in cyanobacteria

Summary

The bacterial RNA-binding protein Hfq functions in post-transcriptional regulation of gene expression. There is evidence in a range of bacteria for specific sub-cellular localization of Hfq, however the mechanism and role of Hfq localization remain unclear. Cyanobacteria harbour a subfamily of Hfq that is structurally conserved but exhibits divergent RNA-binding sites. Mutational analysis in the cyanobacterium *Synechocystis* sp. PCC 6803 revealed that several conserved amino acids on the proximal side of the Hfq hexamer are crucial not only for Hfq-dependent RNA accumulation but also for phototaxis, the latter of which depends on type IV pili. Co-immunoprecipitation and yeast two-hybrid analysis show that the secretion ATPase PilB1 (a component of the type IV pilus base) is an interaction partner of Hfq. Fluorescence microscopy revealed that Hfq is localized to the cytoplasmic membrane in a PilB1-dependent manner. Concomitantly, Hfq-dependent RNA accumulation is abrogated in a Δ*pilB1* mutant, indicating that localization to the pilus base via interaction with PilB1 is essential for Hfq-function in cyanobacteria.

Introduction

The RNA chaperone Hfq is conserved in a wide range of bacterial phyla and plays an important role in post-transcriptional gene regulation (reviewed in Vogel and Luisi, 2011). It belongs to the family of Sm/Sm-like proteins (Lsm), and is structurally and functionally related to the distant archaeal and eukaryotic homologs. The proximal and the distal faces of the characteristic hexameric torus structure of Hfq contribute to its RNA-binding capabilities, although both faces possess a distinct binding site

with divergent sequence specificities (Schumacher *et al.*, 2002; Link *et al.*, 2009). Additionally, charged residues on the lateral surface of the hexamer are involved in RNA binding (Sauer *et al.*, 2012). Hfq binds to *trans*-encoded sRNAs as well as their target mRNAs, thus facilitating base pairing between the two strands with limited sequence complementarity. Hfq-binding and/or duplex formation may subsequently regulate gene expression at the level of RNA stability or translation (Vogel and Luisi, 2011).

Apart from binding RNA, Hfq is known to interact with protein partners many of which are involved in RNA metabolism. In *E. coli* Hfq recruits RNase E for the degradation of bound RNAs (Morita *et al.*, 2005) and regulates polyadenylation dependent RNA decay in a complex with polynucleotide phosphorylase and poly(A) polymerase (Mohanty *et al.*, 2004). Hfq mediates antitermination by forming a complex with Rho (Rabhi *et al.*, 2011) and there is evidence that Hfq associates with the RNA polymerase via the ribosomal protein S1 (Sukhodolets and Garges, 2003; Windbichler *et al.*, 2008) in *E. coli*. Argaman *et al.* (2012) demonstrated that RelA, the regulator of bacterial stringent response, enhances multimerization of Hfq monomers and RNA binding by an unknown process. Furthermore, a large scale analysis revealed that Hfq directly or indirectly interacts with over 30 proteins of diverse (multi-protein complexes) (Butland *et al.*, 2005). Different studies regarding the subcellular localization of Hfq in *E. coli* produced ambiguous data and confirmed localization in the cytoplasm and the nucleoid (Kajitani *et al.*, 1994; Azam *et al.*, 2000) or mainly to the cell membrane (Diestra *et al.*, 2009). However, it remains unclear which factors contribute to the specific subcellular and probably dynamic localization of Hfq in the bacterial cell.

Cyanobacteria are organisms conducting a phototrophic lifestyle. They perform oxygenic photosynthesis and are evolutionarily related to chloroplasts. The sequences of cyanobacterial Hfq orthologues are highly conserved among all cyanobacteria but quite distinct from those of other bacteria. Nevertheless, crystal structures of cyanobacterial Hfq homologs revealed that they retain a perfect Sm-fold and form the typical homohexameric torus structure (Bøggild *et al.*, 2009). However, the electrochemical surface is very distinct and the Hfq homolog of *Synechocystis* sp. PCC 6803 (hereafter *Synechocystis*) binds known enterobacterial sRNAs with very low affinity and is not able to complement an *E. coli hfq* mutant (Bøggild *et al.*, 2009), which raises the question about conservation of the described functions and structure of Hfq in cyanobacteria. Compared with the wide-ranging effects of inactivation of *hfq* in other bacteria, genetic inactivation of the *hfq* gene in different cyanobacteria resulted in relatively restricted phenotypes. In the filamentous nitrogen-fixing cyanobacterium *Nostoc* sp. PCC 7120, Hfq was found to be important for nitrate and nitrite assimilation (Puerta-Fernández and Vioque, 2011). A *Synechocystis* Δ*hfq* mutant showed a defect in type IV pilus (T4P) biogenesis and a decreased accumulation of several mRNAs centred on alterations in transcripts that are under the control of a cAMP receptor protein (CRP)-like transcription factor (SyCRP1) (Dienst *et al.*, 2008) which is involved in T4P biogenesis (Yoshimura *et al.*, 2002). Using T4P, *Synechocystis* exhibits flagella-independent “twitching motility” and is capable of phototaxis i.e. directed movement along a light gradient (Bhaya *et al.*, 1999). Mutation of *hfq* in *Synechocystis* consequently leads to a loss of motility and phototactic response (Dienst *et al.*, 2008). Though many sRNAs have been reported for *Synechocystis* (Georg *et al.*, 2009; Mitschke *et al.*, 2011) little is known about their

roles in cellular functions. Moreover, neither binding of these sRNAs to Hfq nor involvement of protein interaction partners in Hfq-function has been demonstrated for cyanobacterial Hfq proteins.

Considering the divergent properties of cyanobacterial Hfq homologs compared to other bacteria, we elucidated which single amino acid residues are important for Hfq-function in *Synechocystis*. These are very different from standard Hfq proteins and are located outside the non-conserved putative RNA binding pocket. As we suppose that the RNA-binding properties of the cyanobacterial Hfq are very weak, if existing at all, we focused on identification of protein interaction partners. Here, we found that Hfq is localized to the cytoplasmic membrane by binding to the pilus subunit PilB1. Most importantly, we conclude that function of Hfq depends on its correct localization.

Results

Sequence conservation of cyanobacterial Hfq homologs

Hfq homologs in cyanobacteria were originally discovered by BLAST search (Valentin-Hansen *et al.*, 2004) but show great divergence from other bacterial Hfq proteins. To better address distribution and conservation of cyanobacterial Hfq proteins, we did a new BLAST search including the novel CyanoGEBA dataset (Shih *et al.*, 2013). Sequence analysis revealed that 115 out of 132 cyanobacterial genomes harbour an *hfq* homolog (Fig. S1). Obligate symbionts and strains from the genus *Prochlorococcus* mainly lack a discernible homolog. Examining the amino acid conservation with ConSurf (Ashkenazy *et al.*, 2010), it is remarkable that all of the

most conserved residues contribute to the surface of the proximal site (Fig. 1A, B). Around the entire torus, residues from the N-terminal α-helix and the ultraconserved WQD-motif form an area of conserved amino acids which encloses the proximal RNA binding site. We will refer to this area as the proximal outer ring. On the other hand, structurally conserved residues contributing to the proximal (Schumacher *et al.*, 2002; Bøggild *et al.*, 2009), distal (Link *et al.*, 2009) and lateral (Sauer *et al.*, 2012) RNA binding sites are generally not highly conserved among cyanobacterial Hfq proteins (Fig. 1A, B and Fig. S2).

The classical RNA-binding pockets seem not to be essential for Hfq function in Synechocystis

The lack of conservation on sequence level and an unfavourable surface charge (Bøggild *et al.*, 2009) make the known RNA-binding pockets of Hfq an unlikely candidate for RNA-binding in *Synechocystis*. To verify this assumption, we constructed different Hfq variants carrying single-amino-acid substitutions of residues potentially involved in RNA-binding mainly because of its conserved position in the hexamer as deduced from structural information (Bøggild *et al.*, 2009). These mutated Hfq variants were introduced into a Δ*hfq* mutant strain and tested for their ability to complement the mutant phenotype. We used the conjugative shuttle vector pVZ321 to express the Hfq derivatives Q15R (conserved residue on the proximal face of cyanobacterial Hfq proteins), G31N (altering the distal binding site), T43D and D44K (altering the proximal binding site) (Fig. 1A) under the control of the native *hfq* promoter in a Δ*hfq* strain. In contrast to the non-motile Δ*hfq* strain, all four strains expressing mutant Hfq variants showed positive phototaxis towards unidirectional

white light comparable to the wild type (Fig. 1C). As a control we also studied accumulation of the sRNA SyR14 in the RNA-binding pocket mutants. This sRNA identified in dRNA-seq (Mitschke *et al.*, 2011) shows altered transcript accumulation in cells lacking Hfq due to an unknown mechanism. A supposed processing product of SyR14, which accumulates in the wild type, was not detected in the Δ*hfq* mutant and overall transcript abundance was reduced (Fig. 1D). In contrast to the altered SyR14 accumulation in Δ*hfq*, it is clearly seen that the putative RNA-binding pocket mutants accumulated wild-type levels of SyR14 and of its processing product (Fig. 1D). In addition, we purified a 3xFLAG tagged version of Hfq from cell extracts in order to identify RNAs that are bound to Hfq (Fig. S4B). However, neither SyR14 nor other known Hfq-dependent sRNAs were found to be enriched in Hfq purifications. Taken together, our results as well as surface charge distribution imply that the putative RNA-binding pockets are not crucial for the function of Hfq in *Synechocystis* and most likely do not bind RNA.

Residues on the proximal outer ring are important for Hfq function

In order to identify amino acid residues that are important for Hfq function, we performed random mutagenesis of the *hfq* gene sequence by error-prone PCR, followed by screening for motility. We used the cyanobacterial expression vector pUR (Wiegard *et al.*, 2013) containing an inducible promoter and a sequence encoding a 3xFLAG-tag for detection of the protein. We had to use this mobilisable vector because the Δ*hfq* mutant lost its natural competence for transformation due to the loss of T4P (Dienst *et al.*, 2008). The pUR-*hfq* derivatives harbouring the mutagenised *hfq* sequences were then transferred to Δ*hfq* mutant cells via

conjugation and exconjugants were screened on low percentage agar plates under inducing conditions for motility. Most colonies showed the wild-type motile phenotype, meaning that either the introduced *hfq* sequence was not mutated in these clones or the mutation did not lead to a non-functional protein. In summary 116 non-motile clones that did not complement the Δ*hfq* phenotype were subjected to Western Blot analysis using an antibody directed against the 3xFLAG tag that was fused to Hfq. In protein extracts of 38 of these clones we detected the Hfq protein in immunoblot analysis (Fig. S5), verifying the stability of the mutated protein variants. Sequence analysis revealed that 8 clones had single mutations leading to one amino acid residue change. In the other 30 clones that were not further analyzed *hfq* was mutated at more than one site, leading to two or more amino acid changes. Mutations led to following single amino acid replacements: R39H, Q15H, D42N, R3S, P9T, W40R, I18F, V58E (Fig. 1A, B). For seven mutants complete loss of motility was validated by phototaxis assays (Fig. 1E) and additionally, these mutants showed a defect in the accumulation and processing of SyR14 (Fig. 1F). Contrary to the initial screening the R3S mutant could partially complement the Δ*hfq* phenotype showing reduced motility in the phototaxis assay and a faint signal for the SyR14 processing product, albeit the overall transcript accumulation was comparable to the non-functional mutants. Interestingly, Q15H could not complement the Δ*hfq* phenotype, while the above mentioned Q15R mutant was indiscernible from the wild type. Most of the critical residues found in this approach are highly conserved among cyanobacteria and all (except V58) are congruent with the proximal outer ring while none of the critical residues contribute to the distal surface of Hfq, highlighting the functional importance of the proximal surface area (Fig. 1B).

Hfq interacts with the T4P secretion ATPase PilB1

Given the fact that binding of RNA to cyanobacterial Hfq proteins with high affinity could not be shown so far (Bøggild *et al.*, 2009), and our observations that Hfq-dependent RNAs were either not detected or enriched in Hfq purifications (Fig. S3B) and that the proximal and distal RNA-binding pockets most probably are not required for Hfq function, we hypothesized that Hfq may function differently from canonical bacterial Hfq proteins. We reasoned that the critical residues contributing to a large, highly conserved surface area on the proximal side of Hfq constitute an interface for protein interaction. To obtain a better understanding of the mode of action of Hfq, we carried out co-immunoprecipitation experiments in order to find protein interaction partners which may be important for Hfq function. Therefore we generated a Δ*hfq* strain expressing an N-terminally 3xFLAG tagged Hfq variant (Hfq-3xFLAG) under control of the *petJ* promoter from a neutral site in the chromosome (Kuchmina *et al.*, 2012). The fusion protein was shown to be functional by Northern blot analysis and phototaxis assays (Fig. S3B, C) and was purified from the solubilised whole cell lysate with immobilized anti-M2 antibody and separated on SDS-PAGE. In the Hfq-3xFLAG elution fraction an abundant band migrating just below the 75 kDa marker could be detected that was absent in the control (Fig. S6). The corresponding protein could be unambiguously identified as the 75.1 kDa protein PilB1 (encoded by *slr0063*) by mass spectrometry. Intriguingly, PilB1 is the pilus assembly ATPase necessary for pilus extension in *Synechocystis* and thus, Δ*pilB1* cells are non-motile (Yoshihara *et al.*, 2001). Therefore, if Hfq is also important for PilB1 function, this

could account for the absence of pili on the cell surface and the non-motile phenotype of the Δ*hfq* mutant.

PilB1 is a member of the secretion ATPase superfamily which typically shows a two domain architecture with a membrane-facing N-terminal domain and a cytoplasm-facing C-terminal domain with a variable C2 subdomain at the C-terminus (Yamagata and Tainer, 2007). We observed that nearly all cyanobacterial PilB homologs possess a conserved C-terminal region of ~ 40 amino acids with four invariable C residues in a CXXC-X_{10}-CPYC motif which is likely to coordinate a metal ion and resembles a zinc finger domain (Fig. 2A; Fig. S7). Moreover, the only strains of the genus *Prochlorococcus* harbouring an Hfq homolog (MIT 9313, MIT 9303; Fig. S1) are likewise the only two strains of the genus encoding a PilB protein with this putative zinc-finger domain. To address the significance of this domain and determine the Hfq-PilB1 interaction more accurately, we assessed the interaction of Hfq with different PilB1 domains in a yeast two-hybrid system (Fig. 2B). Employing Hfq as prey we screened for interaction with bait vectors containing either the N-terminal (PilB1-N; 1-366) or the C-terminal (PilB1-C; 367-672) PilB1 domain, the putative zinc-finger domain (PilB1-C2; 633-672) or a mutated variant with the conserved C substituted for A residues (PilB1-C2mut). Selective growth on adenine minus plates shows that Hfq interacts with both itself and PilB1-C, whereas no interaction was detected with PilB1-N. In particular, Hfq showed specific interaction with PilB1-C2 alone. Substitution of the conserved cysteines which allegedly abolishes the assumed metal coordinating abilities of this domain also abrogates protein interaction. Subsequently, we investigated the interaction of the non-functional Hfq variants with single amino acid substitutions (Fig. 1) with the C-

terminal domain of PilB1, and additionally tested their ability to interact with a wild-type Hfq bait protein. Fig. 2C confirms direct binding of R39H, Q15H, D42N, P9T, W40R and I18F variants to the wild-type Hfq protein implying that these mutations do not interfere with Hfq hexamerization. By contrast, the V58E mutation abrogates subunit interaction, which is in accordance with the role of the Sm2 motive in subunit contact. Regarding the Hfq-PilB1 interaction we found that direct binding of Hfq to PilB1-C as well as PilB1-C2 is lost in all mutant variants apart from R39H and Q15H. These results confirm the Hfq-PilB1 interaction detected by co-immunoprecipitation and suggest that Hfq binds to the C-terminal domain of PilB1 via conserved functionally important residues on the proximal outer ring.

Hfq is localized to the cell periphery

To determine if Hfq is indeed binding to the pilus base in *Synechocystis* we first tested its localization employing fluorescence microscopy. To begin with, we overexpressed N- and C-terminal Hfq-eYFP fusion proteins (eYFP-Hfq and Hfq-eYFP, respectively) using a conjugative vector and checked if the constructs could complement the Δ*hfq* phenotype. Northern blot analysis (Fig. 3A) showed that only the strain expressing the Hfq-eYFP fusion protein accumulated SyR14 and the putative processing product comparable to the wild type. In agreement with this result, the strain also showed phototactic motility (Fig. 3B), while the eYFP-Hfq fusion was not able to re-establish motility in Δ*hfq*. We then used cells grown on phototaxis plates for fluorescence microscopy. High intensity eYFP-fluorescence could be observed in both mutant strains (Fig. 3C), clearly indicating that eYFP-Hfq fusion is expressed but non-functional. Most importantly, only the functional Hfq-eYFP showed

distinct localization (Fig. 3C, left panel). In this strain we could observe small fluorescent spots along the entire cell periphery of the coccoid cells. In addition, we often detected one large bright spot in each cell, which also appeared to be located at the cell periphery, while very little fluorescence was detected in the cytoplasm. In contrast, we observed no membrane localization in the strain expressing non-functional eYFP-Hfq, where fluorescence was uniformly distributed in the cytoplasm. Hence, we conclude that Hfq is specifically localized to the cell membrane in *Synechocystis*. Localization to the cell membrane is disrupted by an eYFP tag at the N-terminus, and this loss of Hfq localization correlates with loss of phototaxis and incorrect processing of SyR14. To further explore the connection between localisation and function we analyzed the localisation of some of the non functional Hfq variants by constructing C-terminal eYFP fusion proteins. We chose the Hfq variants P9T, I18F and D42N (as one of the mutants from the highly conserved WQD motif) because they retained the ability to interact with wild-type Hfq monomers but showed no interaction with PilB1 in the yeast two-hybrid analysis (Fig. 2C). As shown in the fluorescence images (Fig. 4) localization in all strains expressing mutant Hfq variants was altered. Mutants I18F and D42N show very bright dispersed fluorescence in the cytoplasm, whereas in mutant P9T only one bright spot is visible. Importantly, the accumulation of small fluorescent spots along the cell periphery, as seen for wild-type Hfq-eYFP is clearly missing in P9T and I18F.

Hfq-PilB1 interaction is crucial for the localization of Hfq, phototactic motility and transcript accumulation.

Thus far, we have shown that Hfq localizes to the cell periphery and co-purifies with PilB1 which is supposed to interact with the pilus base at the cytoplasmic membrane. To investigate whether the Hfq-PilB1 interaction is a prerequisite for the correct localization of Hfq, we analysed the localization of Hfq-eYFP in a *pilB1* knockout strain. Fluorescence microscopy revealed that the localization of multiple small fluorescence spots along the cell periphery is completely lost in the Δ*pilB1* background (Fig. 5A). Instead, Hfq-eYFP is concentrated in very intense spots, usually no more than one per cell and usually (but not always) at the cell periphery. The change in Hfq-eYFP distribution is quantifiable and highly significant. In the Δ*pilB1* background, the mean number of Hfq-eYFP spots per cell observed in our confocal optical sections decreases from about 3.3 to 0.9, while the mean spot intensity increases by a factor of >4. In both cases, t-tests gave *p*-values $<10^{-10}$. Together with the results from the co-immunoprecipitation experiment, this observation supports our hypothesis that Hfq is localized to the pilus base at the cytoplasmic membrane via an interaction with PilB1.

To explore if the localization of Hfq and/or its interaction with PilB1 is important for its function, we subsequently analyzed SyR14 accumulation in Δ*pilB1/*Δ*hfq* x Hfq-eYFP as well as in Δ*pilB1* and Δ*pilC* strains. We included the Δ*pilC* mutant in the analysis because in the current model for T4P assembly it is believed that PilB exerts its role in pilus extension by interacting with the integral membrane protein PilC (Crowther *et al.*, 2004). Interestingly, none of the strains with inactivated *pilB1* or *pilC*

genes accumulated the SyR14 processing product in Northern blot experiments (Fig. 5B). Also, in accordance to the fundamental role PilB1 and PilC play in the assembly of T4P, these mutants showed no motility in a phototaxis assay (Fig. 5C). These findings support the notion that the direct interaction between PilB1 and Hfq and/or the localization to the pilus base is critical for Hfq function.

As a further test for direct interaction between Hfq and PilB1, we simultaneously visualised PilB1-sfGFP and Hfq-eYFP expressed in the *ΔpilB1* background (Fig. 6). Phototaxis experiments verified that the C-terminally sfGFP tagged PilB1 protein is functional as it complements the *ΔpilB1* mutant (Fig. S8A). Using appropriate settings on the confocal microscope we were able to visualise sfGFP and eYFP simultaneously, with no significant cross-detection or interference from the fluorescence of the photosynthetic pigments (Fig. S8B). As would be expected, PilB1-sfGFP fluorescence is strongly concentrated around the periphery of the cell (Fig. 6). The Hfq-eYFP fluorescence around the cell periphery shows partial co-localisation with PilB. Some concentrations of PilB-sfGFP fluorescence correspond precisely (at optical resolution) to concentrations of Hfq-eYFP fluorescence, but it is also possible to find concentrations of Hfq-eYFP fluorescence without a corresponding spot of PilB-sfGFP fluorescence, and *vice versa* (Fig. 6). Thus our co-localisation results are consistent with a direct PilB1-Hfq interaction, but they indicate that there is not a simple 1:1 association of the two proteins.

Discussion

The proximal outer ring but not the classical RNA-binding pockets are essential for Hfq function in Synechocystis

The RNA binding pocket of Hfq is well conserved in most bacteria, however sequence conservation of the residues surrounding the central cavity is relatively low in cyanobacteria. Here, we show that mutations of residues (T43, D44) contributing to the structurally conserved proximal RNA binding pocket do not compromise function of the cyanobacterial Hfq protein. Furthermore, none of the other residues (R59, L60, A61) implicated in RNA-binding around the central cavity appear to be critical for function, since mutations in these residues were not found in our random mutagenesis screen. This would be in accordance with the absence of the archetypal Sm2 signature sequence [*Y/F*]KHAI of Hfq in cyanobacteria (Bøggild *et al.*, 2009). Other bacterial Hfq homologs have highly similar or identical residues in this region (Mikulecky *et al.*, 2004) and mutations of residues around the central cavity in *E. coli* Hfq showed severe defects in RNA binding and riboregulation *in vivo* and *in vitro* (Mikulecky et al., 2004; Zhang et al., 2013). By contrast, our results show that the proximal RNA-binding pocket around the central cavity that binds preferentially U-rich RNA 3′-ends in Enterobacteria (Sauer and Weichenrieder, 2011) seems not to be involved in Hfq function in *Synechocystis*. Regarding the distal face of the Hfq hexamer, we did not identify any residue contributing to this surface in our screen for non-functional Hfq variants, nor did the G31N mutation abrogate Hfq function. Together with the observed lack of strong conservation of distal face residues (Fig. 1)

this implies that this surface also does not form an essential interaction site for RNA. These results are substantiated by a study showing a very low affinity of two cyanobacterial Hfq proteins for known Hfq-dependent sRNAs from *E. coli* and the inability of the cyanobacterial Hfq protein to complement an *E. coli hfq* mutant strain (Bøggild *et al.*, 2009). Indeed, as we were also unable to detect Hfq-dependent sRNAs in purified Hfq samples, one has reason to generally question the role of *Synechocystis* Hfq as a RNA-chaperone (Fig. S3B). However, we observed a strong correlation between impaired SyR14 processing and motility and therefore we believe that Hfq exerts some of its function at the level of posttranscriptional gene regulation by a so far unknown mechanism.

The proximal outer ring is critical for Hfq-PilB1 interaction

Given that the most conserved residues among cyanobacterial Hfq proteins are found in the proximal outer ring (Fig. 1) and all our deleterious amino acid substitutions were found in this region, we presume that this surface comprises the essential functional site of Hfq. Mutational studies in *E. coli* led to conflicting results regarding the requirement of proximal face residues outside the central cavity for RNA-binding and riboregulation. But for some of these residues a role in stable hexamer formation was suggested (Mikulecky *et al.*, 2004; Zhang *et al.*, 2013). We observed that subunit interaction is abrogated in the V58E mutant (Fig. 2C) and we cannot exclude the possibility that hexamer stability or conformation is altered in some of the other *Synechocystis* Hfq mutants. However, mutation of residues contributing to the proximal outer ring did not disturb monomer interaction in yeast

two-hybrid analysis (Fig. 2C) and therefore we conclude that loss of function in these Hfq variants cannot generally be attributed to compromised hexamer formation. Instead, we could demonstrate that Hfq interacts with PilB1 and that this interaction was lost in the Hfq variants P9T, I18F, W40R and D42N. Only two mutations (R39H and Q15H) disturb Hfq function but not binding to PilB1. Three Hfq mutants (P9T, I18F and D42N) were further analyzed by fluorescence microscopy. In these mutants Hfq was found to be incorrectly localized (Fig. 4). The mean number of spots per cell in the P9T mutant resembles the fluorescence distribution in the Δ*pilB1* mutant, implying that Hfq-PilB1 interaction is lost in this mutant. The diffuse eYFP fluorescence in the cytoplasm of the I18F and D42N mutants in addition to the occurrence of bright spots in some cells indicates that Hfq-PilB1 interaction is also lost. Taking into account that the N-terminal (proximal facing) eYFP–Hfq fusion protein also was non-functional and did not localize to the cell membrane, we hypothesize that the proximal outer ring of the Hfq hexamer comprises the interface for PilB1 interaction and that this interaction is critical for Hfq function. Interestingly, we observed complete or partial loss of aggregation of Hfq in the form of bright fluorescent spots in several non-functional Hfq variants. This could be due to disturbed polymerisation into higher order structures which were demonstrated for *E. coli* Hfq and other Sm-like proteins (Arluison *et al.*, 2006).

Localization of Hfq to the pilus base

The most novel aspect arising from this study is the interaction of Hfq with the secretion ATPase PilB1 and the consequent localization of Hfq to the cell periphery. Furthermore, this interaction is critical both for the accumulation of Hfq-dependent

transcripts and for phototactic motility. Direct interaction has been shown for homologs of PilB and the membrane-integral pilus platform protein PilC in *E. coli* (Crowther *et al.*, 2004) and localization of *Pseudomonas aeruginosa* PilB to the cytoplasmic membrane is abolished in a Δ*pilC* background (Chiang *et al.*, 2005). Assuming a similar interaction of PilB1 and PilC in *Synechocystis*, Hfq would be localized to the cytoplasmic membrane by interaction with PilB1 bound to PilC. We found that Hfq-dependent processing of SyR14 is abolished in the *Synechocystis* Δ*pilC* strain as well as in the Δ*pilB1* strain. This indicates that interaction with PilB1 is not sufficient for Hfq function: the whole complex must also be correctly localized at the pilus base through interaction with PilC. While we cannot exclude the involvement of other residues, our results implicate that the Hfq-PilB1 interaction is mediated primarily by the small (40 amino acids) C-terminal zinc-finger-like domain of PilB1. Importantly, the high degree of sequence conservation of this domain in conjunction with the noted co-occurrence with Hfq implies an evolutionarily conserved mechanism of Hfq-PilB interaction in cyanobacteria.

Interaction of Hfq with the T4P pilus base is consistent with the absence of pili on the cell surface in the Δ*hfq* strain (Dienst et al. 2008). Considering that we have no evidence for specific RNA-Hfq interaction in *Synechocystis*, a direct role of Hfq in pilus assembly would be the simplest explanation for the observed phenotype. However, it is clear that Hfq must have additional functions beyond pilus assembly since Δ*hfq* mutant cells display reduced transcript accumulation of a set of mRNAs (Dienst et al. 2008) and sRNAs (Fig. S4A). Among them are the transcripts of minor pilins (PilA9-11) and cell surface components (Slr1667 and Slr1668) that are under the control of the cAMP-dependent transcription factor SyCRP1, known to be

involved in phototactic motility (Yoshimura *et al.*, 2002; Yoshimura *et al.*, 2010). Given our strong evidence for direct interaction between Hfq and PilB1 and the importance of correct Hfq localization we suggest that Hfq could facilitate a differential subcellular accumulation and translation of transcripts encoding gene products that are involved in phototactic motility or require PilB1 for translocation through the T4P.

A vast number of Hfq-dependent sRNAs are involved in the regulation of outer membrane proteins (Vogel and Papenfort, 2006) and there are reports suggesting that Hfq-dependent riboregulation of secreted and membrane proteins takes place in close proximity to the cytoplasmic membrane. For example, in *E. coli* Hfq is localized to the cell membrane (Diestra *et al.*, 2009) and the Hfq/SgrS-dependent regulation of the *ptsG* mRNA is dependent on the localization of the transcript to the cytoplasmic membrane coupled with the insertion of the nascent peptide (Kawamoto *et al.*, 2005). A recent study in *Salmonella* demonstrated that short AU-rich sequences in the 5'-UTR of *gtgA*, *gogB* and *sseL* are sufficient for the translocation of reporter proteins via a type 3 secretion system in a wild-type strain but not in a Δ*hfq* mutant (Niemann *et al.*, 2013). Here, the abrogation of protein secretion in Δ*hfq* was not a consequence of a defective type 3 secretion apparatus or decreased protein expression and *gtgA* mRNA was shown to interact with Hfq. Additionally, *E. coli* Hfq has been copurified with proteins involved in protein translocation, like FliS and SecA (Arifuzzaman *et al.*, 2006). Thus, we speculate that Hfq might play an important function in posttranscriptional regulation as part of a membrane-associated protein complex involved in protein translocation in different bacteria.

Experimental procedures

Bacterial strains and growth conditions

Liquid cultures of *Synechocystis* wild-type (originally obtained from S. Shestakov, Moscow State University, Russia) and mutant strains were grown in BG11 medium (Rippka *et al.*, 1979) supplemented with 10 mM TES buffer (pH 8.0) at 30°C under white light of 50 µmol photons m^{-2} s^{-1} and constant shaking. For induction of the P*petJ* promoter $CuSO_4$ was omitted from the medium.

Mutagenesis and plasmid construction

The construction of the Δ*hfq* mutant was described in Dienst *et al.,* 2008 (see also Fig. S3A). Primers used for mutant constructs are listed in the Supporting Information. For site directed mutagenesis we used an 1111 bp fragment containing the *hfq* gene together with its promoter and terminator sequences (Dienst *et al.*, 2008) ligated into the pDrive vector (Qiagen) using PstI and SalI restriction sites. The resulting plasmid (pDrive-*hfq*) was used as a template for two separate PCR reactions each involving a primer harbouring the mutated sequence (Q15R: a44g, a44g_as; G31N: g91a_g92a_g93c, g91a_g92a_g93c_as; T43D: a127g_c128a, a127g_c128a_as, D44K: g130a_t132a, g130a_t132a_as) and a vector primer (M13fw or M13rev). These two DNA fragments were used in a third PCR reaction using both vector primers. The resulting PCR fragment was subcloned into pJET vector (Fermentas). The pJET vector was then cleaved by PstI and SalI and the fragment containing the mutagenised *hfq* sequence together with its promoter and terminator sequences was ligated into the respective restriction sites of the conjugative vector pVZ321 (pVZ321-*hfq#AA*, Fig. S3B). The pVZ321-*hfq* vector was

transferred to *Synechocystis* 6803 Δ*hfq* mutant cells via conjugation (Zinchenko *et al.*, 1999) and exconjugants were selected on 40 µg ml^{-1} Km. For construction of randomly mutagenised *hfq* sequences we again used the pDrive-*hfq* vector as a template. An error prone PCR reaction (5.0 mM $MgCl_2$, 0,2 mM dATP and dGTP, 1 mM dCTP and dTTP, 0.3 mM $MnCl_2$, 5U Dream Taq (Fermentas) was performed using the primer pair (hfq-EcoRI-fw and hfq-BamHI-rev) and the PCR products bearing the coding sequence of *hfq* flanked by EcoRI and BamHI restriction sites were ligated into the pJET vector. Plasmid DNA was isolated from all obtained recombinant *E. coli* colonies in one sample and subjected to digestion with EcoRI and BamHI. The DNA fragments were then ligated into EcoRI and BamHI restriction sites of the pUR expression vector (Wiegard *et al.*, 2013). This led to a mobilisable plasmid harbouring randomly mutated *hfq* sequences flanked at the 5`end by the copper sensitive promoter P*petJ* and a 3xFLAG sequence and at the 3`end by the *oop* terminator from phage Lambda (pUR-*hfq#AA*, Fig. S3C).

Insertion of Hfq-3xFLAG in a neutral locus of the Δ*hfq* strain was carried out using a similar strategy as for the Ycf34-3xFLAG strain (Wallner *et al.*, 2012). Briefly, the *hfq* ORF and the 200nt downstream sequence was amplified using primers hfq-NdeI-fw and hfq-BglII-rev and the PCR-fragment was subcloned into the pJET vector. It was excised with NdeI and BglII and ligated into a modified pSK9 vector (Kuchmina *et al.*, 2012) (the Km resistance cassette from pUC4K vector was excised with EcoRI and ligated into the psK9 EcoRI site, disrupting the chloramphenicol resistance cassette) resulting in pSK9-Hfq. Subsequently oligonucleotides containing the 3x-FLAG epitope (FLAG-fw and FLAG-rev) were hybridized and ligated into the pSK9-

Hfq vector, linearised with NdeI (pSK-3xFLAG-*hfq*, Fig. S3D). This construct was introduced into Δ*hfq* mutant cells by electroporation (Thiel and Poo, 1989).

The *hfq* gene was amplified using primers hfqYFPNde and hfqYFPXho and the gene encoding eYFP was amplified from pEYFP-His_6-Sp^R plasmid described in (Birungi *et al.*, 2010) using primers eYFPXho and eYFPBglII generating NdeI, XhoI and BglII restriction sites at the 5` and 3`ends, respectively. The fragments were subcloned the psk9 based expression vector pSDC01 (Savakis *et al.*, 2012) to generate a C-terminal YFP tagged Hfq fusion. A PvuII fragment bearing the expression cassette together with eYFP tagged *hfq* was then ligated into a modified pVZ321 vector (Zinchenko et al. 1999) where the chloramphenicol resistance cassette was exchanged by the *aadA* gene conferring streptomycin resistance (pVZ-*hfq*-eYFP, Fig. S3E). To generate the eYFP tagged Hfq variants carrying singe amino acid substitutions the same strategy was used but the mutated *hfq* sequence from the clones generated by error prone PCR was used. For N-terminal fusion of eYFP to *hfq* the eYFP gene was amplified using the primer pair NdeI-eYFP-fw and eYFP-EcoRI-rev; the *hfq* sequence was amplified with primers hfq-Eco-fw and hfq-BamHI-rev generating EcoRI and BglII restrictions sites at the ends and both fragments were subsequently ligated into the pVZ321 based conjugative expression vector pUR allowing expression from the P*petJ* promoter (pVZ-eYFP-*hfq*, Fig. S3F). Δ*pilB1* and Δ*pilC* mutants were generated by transformation of the wild-type strain with genomic DNA of *slr0063::zeo* or *pilC:aadA* strains obtained from Roman Sobotka (Department of Phototrophic Microorganisms, Academy of Sciences, Trebon).

To generate a C-terminal GFP tagged PilB1 fusion protein we amplified the sequence encoding “superfolder” sfGFP fused to a 12 amino acid linker from plasmid

pXG10-SF (Corcoran *et al.*, 2012) using primers XhoI-L-sfGFP-fw and BglII-L-sfGFP-rev and the *pilB1* gene using primers NdeI-pilB-fw and XhoI-pilB-rev. These fragments were cloned into the respective NdeI/XhoI and XhoI/BglII restriction sites of vector pSDC01 which was subsequently used to transform *Synechocystis*.

Motility assays

Phototactic movement was analysed on 0.5% (w/v) BG11 agar plates with 0.2% glucose added. Cell suspensions were spotted on the plates and incubated for 2-3 days under diffuse white light (50 µmol photons m^{-2} s^{-1}) before being placed into non-transparent boxes with an one-sided opening (>5 µmol photons m^{-2} s^{-1}) for 10 days.

RNA isolation and northern blot hybridization

Approximately 30 ml of *Synechocystis* liquid cultures were collected at an OD_{750nm} of 0.6-0.8 by quenching on ice and immediate centrifugation at 4 °C. RNA was isolated using the PGTX method (Pinto *et al.*, 2009) with an additional phenol/chloroform/isoamyl alcohol (25:24:1 v/v) extraction preceding the RNA precipitation. Total RNA was diluted in 30 µl H_2O and 5-10 µg were separated by electrophoresis on 10% denaturing urea polyacrylamide gels and blotted onto Roti-Nylon plus (Roth) membranes. Hybridization probes were generated either by *in vitro* transcription of PCR fragments from the T7 promoter in the presence of [α-^{32}P]UTP using the T7 polymerase Maxiscript kit (Ambion) or by labeling DNA oligonucleotides with [γ-^{32}P]ATP using T4 polynucleotide kinase (Fermentas). Signals were detected and analysed on a Personal Molecular Imager FX (Bio-Rad). All DNA oligonucleotides are listed in the table at the end of this section.

Yeast two-hybrid analysis

The yeast two-hybrid analysis was carried out as described previously (Watanabe *et al.*, 2007). The DNA fragments of *hfq* and *pilB1* were amplified from genomic DNA of a *Synechocystis* wild-type strain or plasmid DNA in case of the Hfq variants carrying single amino acid substitutions and cloned into pGBTK, a GAL4 DNA-binding domain fusion vector, or pGAD424, a GAL4 activation domain fusion vector, respectively. Bait-prey pairs for specificity were streaked onto SC-LW and -LWA plates and incubated for 6 days. Primers for cloning are listed in the Supporting Information.

Fluorescence microscopy

Fluorescence micrographs were recorded at room temperature (20°C) using a Leica TCS SP5 laser-scanning confocal microscope. For visualisation of YFP in single-labelled cells, excitation was at 496 nm and emission was recorded simultaneously at 520-540 nm (for eYFP) and 670-720 nm (for chlorophyll, showing the location of the thylakoid membranes). For co-localisation of GFP and YFP in dual-labelled cells, sequential images were recorded with excitation at 488 nm, emission 503-515 nm (for GFP) and excitation at 514 nm, emission at 520-540 nm (for YFP). Controls with single-labelled cells show that there is no significant cross-detection of GFP and YFP with these wavelength settings (Supplementary Fig. S8B). For all images, a 63x oil-immersion objective lens (numerical aperture 1.4) was used. The confocal pinhole was set to give an optical section in the *z*-direction of about 1 µm. Cells were taken from agar plates, resuspended in growth medium and then droplets of the cell suspension were adsorbed onto fresh BG11 agar plates. When the liquid had dried, small blocks of agar with the cells on the surface were pressed onto glass cover-slips

and mounted in a custom-made sample holder. Fluorescence intensities were quantified with ImageJ software (National Institutes of Health). Statistical tests were with SigmaPlot 10.0 software (Jandel Scientific).

Acknowledgements

We thank Markéta Foldynová and Roman Sobotka (Department of Phototrophic Microorganisms, Academy of Sciences, Trebon) for generously providing Δ*pilB1* and Δ*pilC* mutant constructs. We also thank Seth Axen and Cheryl Kerfeld (DOE Joint Genome Institute) for very helpful discussions on the Hfq structure and Wolfgang Hess (University of Freiburg) and Cynthia Sharma (University of Würzburg) for analyzing and discussing transcriptomic data. This work was supported by the DFG priority program SPP1258 Sensory and Regulatory RNAs in Prokaryotes (Wi-2014/3-1, 3-2) to A.W. D.J.N. was supported by Queen Mary college studentship.

References

Argaman, L., Elgrably-Weiss, M., Hershko, T., Vogel, J., and Altuvia, S. (2012) RelA protein stimulates the activity of RyhB small RNA by acting on RNA-binding protein Hfq. *Proc Natl Acad Sci* **109**: 4621–4626.

Arifuzzaman, M., Maeda, M., Itoh, A., Nishikata, K., Takita, C., Saito, R., *et al.* (2006) Large-scale identification of protein-protein interaction of *Escherichia coli* K-12. *Genome Res* **16**: 686–691.

Arluison, V., Mura, C., Guzmán, M.R., Liquier, J., Pellegrini, O., Gingery, M., *et al.* (2006) Three-dimensional structures of fibrillar Sm proteins: Hfq and other Sm-like proteins. *J Mol Biol* **356**: 86–96.

Ashkenazy, H., Erez, E., Martz, E., Pupko, T., and Ben-Tal, N. (2010) ConSurf 2010: calculating evolutionary conservation in sequence and structure of proteins and nucleic acids. *Nucleic Acids Res* **38**: W529–W533.

Azam, T.A., Hiraga, S., and Ishihama, A. (2000) Two types of localization of the DNA-binding proteins within the *Escherichia coli* nucleoid. *Genes Cells* **5**: 613–626.

Bhaya, D., Watanabe, N., Ogawa, T., and Grossman, A.R. (1999) The role of an alternative sigma factor in motility and pilus formation in the cyanobacterium *Synechocystis* sp. strain PCC6803. *Proc Natl Acad Sci USA* **96**: 3188–3193.

Birungi, M., Folea, M., Battchikova, N., Xu, M., Mi, H., Ogawa, T., *et al.* (2010) Possibilities of subunit localization with fluorescent protein tags and electron microscopy examplified by a cyanobacterial NDH-1 study. *Biochim Biophys Acta* **1797**: 1681–1686.

Bøggild, A., Overgaard, M., Valentin-Hansen, P., and Brodersen, D.E. (2009) Cyanobacteria contain a structural homologue of the Hfq protein with altered RNA-binding properties. *FEBS J* **276**: 3904–3915.

Butland, G., Peregrín-Alvarez, J.M., Li, J., Yang, W., Yang, X., Canadien, V., *et al.* (2005) Interaction network containing conserved and essential protein complexes in *Escherichia coli*. *Nature* **433**: 531–537.

Chiang, P., Habash, M., and Burrows, L.L. (2005) Disparate subcellular localization patterns of *Pseudomonas aeruginosa* Type IV pilus ATPases involved in twitching motility. *J Bacteriol* **187**: 829–839.

Corcoran, C.P., Podkaminski, D., Papenfort, K., Urban, J.H., Hinton, J.C.D., and Vogel, J. (2012) Superfolder GFP reporters validate diverse new mRNA targets of the classic porin regulator, MicF RNA. *Mol Microbiol* **84**: 428–45.

Crowther, L.J., Anantha, R.P., and Donnenberg, M.S. (2004) The inner membrane subassembly of the enteropathogenic *Escherichia coli* bundle-forming pilus machine. *Mol Microbiol* **52**: 67–79.

Dienst, D., Dühring, U., Mollenkopf, H.J., Vogel, J., Golecki, J., Hess, W.R., and Wilde, A. (2008) The cyanobacterial homologue of the RNA chaperone Hfq is essential for motility of *Synechocystis* sp. PCC 6803. *Microbiology* **154**: 3134–3143.

Diestra, E., Cayrol, B., Arluison, V., and Risco, C. (2009) Cellular electron microscopy imaging reveals the localization of the Hfq protein close to the bacterial membrane. *PLoS One* **4**: e8301.

Georg, J., Voss, B., Scholz, I., Mitschke, J., Wilde, A., and Hess, W.R. (2009) Evidence for a major role of antisense RNAs in cyanobacterial gene regulation. *Mol Syst Biol* **5**: 305.

Kajitani, M., Kato, A., Wada, A., Inokuchi, Y., and Ishihama, A. (1994) Regulation of the Escherichia coli *hfq* gene encoding the host factor for phage Q beta. *J Bacteriol* **176**: 531–534.

Kawamoto, H., Morita, T., Shimizu, A., Inada, T., and Aiba, H. (2005) Implication of membrane localization of target mRNA in the action of a small RNA: mechanism of post-transcriptional regulation of glucose transporter in *Escherichia coli*. *Genes Dev* **19**: 328–338.

Kuchmina, E., Wallner, T., Kryazhov, S., Zinchenko, V. V, and Wilde, A. (2012) An expression system for regulated protein production in *Synechocystis* sp. PCC 6803 and its application for construction of a conditional knockout of the ferrochelatase enzyme. *J Biotechnol* **162**: 75–80.

Link, T.M., Valentin-Hansen, P., and Brennan, R.G. (2009) Structure of *Escherichia coli* Hfq bound to polyriboadenylate RNA. *Proc Natl Acad Sci USA* **106**: 19292–19297.

Mikulecky, P.J., Kaw, M.K., Brescia, C.C., Takach, J.C., Sledjeski, D.D., and Feig, A.L. (2004) *Escherichia coli* Hfq has distinct interaction surfaces for DsrA, rpoS and poly(A) RNAs. *Nat Struct Mol Biol* **11**: 1206–1214.

Mitschke, J., Georg, J., Scholz, I., Sharma, C.M., Dienst, D., Bantscheff, J., *et al.* (2011) An experimentally anchored map of transcriptional start sites in the model cyanobacterium *Synechocystis* sp. PCC6803. *Proc Natl Acad Sci USA* **108**: 2124–2129.

Mohanty, B.K., Maples, V.F., and Kushner, S.R. (2004) The Sm-like protein Hfq regulates polyadenylation dependent mRNA decay in *Escherichia coli*. *Mol Microbiol* **54**: 905–920.

Morita, T., Maki, K., and Aiba, H. (2005) RNase E-based ribonucleoprotein complexes: mechanical basis of mRNA destabilization mediated by bacterial noncoding RNAs. *Genes Dev* **19**: 2176–2186.

Niemann, G.S., Brown, R.N., Mushamiri, I.T., Nguyen, N.T., Taiwo, R., Stufkens, A., *et al.* (2013) RNA type III secretion signals that require Hfq. *J Bacteriol* **195**: 2119–2125.

Pinto, F.L., Thapper, A., Sontheim, W., and Lindblad, P. (2009) Analysis of current and alternative phenol based RNA extraction methodologies for cyanobacteria. *BMC Mol Biol* **10**: 79.

Puerta-Fernández, E., and Vioque, A. (2011) Hfq is required for optimal nitrate assimilation in the Cyanobacterium *Anabaena* sp. strain PCC 7120. *J Bacteriol* **193**: 3546–3555.

Rabhi, M., Espéli, O., Schwartz, A., Cayrol, B., Rahmouni, A.R., Arluison, V., and Boudvillain, M. (2011) The Sm-like RNA chaperone Hfq mediates transcription antitermination at Rho-dependent terminators. *EMBO J* **30**: 2805–2816.

Rippka, R., Deruelles, J., Waterbury, J.B., Herdman, M., and Stanier, R.Y. (1979) Generic assignments, strain histories and properties of pure cultures of cyanobacteria. *J Gen Microbiol* **111**: 1–61.

Sauer, E., Schmidt, S., and Weichenrieder, O. (2012) Small RNA binding to the lateral surface of Hfq hexamers and structural rearrangements upon mRNA target recognition. *Proc Natl Acad Sci USA* **109**: 9396–9401.

Sauer, E., and Weichenrieder, O. (2011) Structural basis for RNA 3'-end recognition by Hfq. *Proc Natl Acad Sci USA* **108**: 13065–13070.

Savakis, P., DeCausmaecker, S., Angerer, V., Ruppert, U., Anders, K., Essen, L.-O., and Wilde, A. (2012) Light-induced alteration of c-di-GMP level controls motility of *Synechocystis* sp. PCC 6803. *Mol Microbiol* **85**: 239–251.

Schumacher, M.A., Pearson, R.F., Møller, T., Valentin-Hansen, P., and Brennan, R.G. (2002) Structures of the pleiotropic translational regulator Hfq and an Hfq-RNA complex: a bacterial Sm-like protein. *EMBO J* **21**: 3546–3556.

Shih, P.M., Wu, D., Latifi, A., Axen, S.D., Fewer, D.P., Talla, E., *et al.* (2013) Improving the coverage of the cyanobacterial phylum using diversity-driven genome sequencing. *Proc Natl Acad Sci USA* **110**: 1053–1058.

Sukhodolets, M. V, and Garges, S. (2003) Interaction of *Escherichia coli* RNA polymerase with the ribosomal protein S1 and the Sm-like ATPase Hfq. *Biochemistry* **42**: 8022–8034.

Thiel, T., and Poo, H. (1989) Transformation of a filamentous cyanobacterium by electroporation. *J Bacteriol* **171**: 5743–5746.

Valentin-Hansen, P., Eriksen, M., and Udesen, C. (2004) The bacterial Sm-like protein Hfq: a key player in RNA transactions. *Mol Microbiol* **51**: 1525–1533.

Vogel, J., and Luisi, B.F. (2011) Hfq and its constellation of RNA. *Nat Rev Microbiol* **9**: 578–589.

Vogel, J., and Papenfort, K. (2006) Small non-coding RNAs and the bacterial outer membrane. *Curr Opin Microbiol* **9**: 605–611.

Wallner, T., Hagiwara, Y., Bernát, G., Sobotka, R., Reijerse, E.J., Frankenberg-Dinkel, N., and Wilde, A. (2012) Inactivation of the conserved open reading frame

ycf34 of Synechocystis sp. PCC 6803 interferes with the photosynthetic electron transport chain. *Biochim Biophys Acta* **1817**: 2016–2026.

Watanabe, S., Kobayashi, T., Saito, M., Sato, M., Nimura-Matsune, K., Chibazakura, T., *et al.* (2007) Studies on the role of HtpG in the tetrapyrrole biosynthesis pathway of the cyanobacterium *Synechococcus elongatus* PCC 7942. *Biochem Biophys Res Commun* **352**: 36–41.

Wiegard, A., Dörrich, A.K., Deinzer, H.T., Beck, C., Wilde, A., Holtzendorff, J., and Axmann, I.M. (2013) Biochemical analysis of three putative KaiC clock proteins from *Synechocystis* sp. PCC 6803 suggests their functional divergence. *Microbiology* **159**: 948–58.

Windbichler, N., Pelchrzim, F. Von, Mayer, O., Csaszar, E., and Schroeder, R. (2008) Isolation of small RNA-binding proteins from *E. coli*: evidence for frequent interaction of RNAs with RNA polymerase. *RNA Biol* **5**: 30–40.

Yamagata, A., and Tainer, J.A. (2007) Hexameric structures of the archaeal secretion ATPase GspE and implications for a universal secretion mechanism. *EMBO J* **26**: 878–890.

Yoshihara, S., Geng, X., Okamoto, S., Yura, K., Murata, T., Go, M., *et al.* (2001) Mutational analysis of genes involved in pilus structure, motility and transformation competency in the unicellular motile cyanobacterium *Synechocystis* sp. PCC 6803. *Plant Cell Physiol* **42**: 63–73.

Yoshimura, H., Kaneko, Y., Ehira, S., Yoshihara, S., Ikeuchi, M., and Ohmori, M. (2010) CccS and CccP are involved in construction of cell surface components in the cyanobacterium *Synechocystis* sp. strain PCC 6803. *Plant Cell Physiol* **51**: 1163–1172.

Yoshimura, H., Yoshihara, S., Okamoto, S., Ikeuchi, M., and Ohmori, M. (2002) A cAMP receptor protein, SYCRP1, is responsible for the cell motility of *Synechocystis* sp. PCC 6803. *Plant Cell Physiol* **43**: 460–463.

Zhang, A., Schu, D.J., Tjaden, B.C., Storz, G., and Gottesman, S. (2013) Mutations in interaction surfaces differentially impact *E. coli* Hfq association with small RNAs and their mRNA targets. *J Mol Biol* **425**: 3678–97.

Zinchenko, V.V., Piven, I.V., Melnik, V.A., and Shestakov, S.V. (1999) Vectors for the complementation analysis of cyanobacterial mutants. *Russ J Genet* **35**: 228–232.

Figure legends

Fig. 1. Sequence conservation and mutational analysis of single amino acid residues. (A) The *Synechocystis* Hfq sequence coloured by sequence conservation among cyanobacterial Hfq homologs. The secondary structure of *Synechocystis* Hfq (PDB ID: 3hfo) is displayed on the top and residues involved in RNA-binding in other bacterial Hfq proteins are marked as followed: ***** putative proximal RNA binding site of *Synechocystis* Hfq determined by structural superposition with the known *S. aureus* RNA-binding site (Schumacher *et al.*, 2002; Bøggild *et al.*, 2009); ● distal RNA binding site seen in the crystal structure of a Hfq-RNA complex in *E. coli* (Link *et al.*, 2009); **+** charged residues contributing to the lateral RNA binding site (Sauer *et al.*, 2012). Amino acid substitutions that did not abolish Hfq function in *Synechocystis* are shown in grey and deleterious substitutions in black. (B) Sequence conservation superimposed on the molecular surface of *Synechocystis* Hfq shows an unilateral arrangement of conserved residues along an “outer proximal ring”. Mutated residues that contribute to the surface area of the Hfq hexamer are indicated. (C) Site directed mutagenesis of specific residues. All mutants showed positive phototaxis towards an unidirectional light source in a phototaxis assay. (D) Northern blot analysis showing that SyR14 transcript accumulation is comparable to the wild type in all mutant strains. (E-F) Random mutagenesis clones with single amino acid substitutions that abolished *Synechocystis* Hfq function and were not able to restore phototactic

motility and SyR14 processing. A sequence alignment of cyanobacterial Hfq proteins is shown in Fig. S1.

Fig. 2. Hfq interacts with the secretion ATPase PilB1. (A) Schematic representation of PilB1 highlighting the domains used in the yeast two-hybrid experiment and showing the sequence motif of the putative zinc-finger domain found in cyanobacterial PilB homologs. The conserved cysteines are marked with red asterisks. (B) Yeast two-hybrid results showing interactions between Hfq and the different domains of PilB1 as indicated above including a C2 variant with the conserved C substituted for A residues (PilB1-C2mut). Empty prey and bait vectors pGAD424 and pGBTK are included as controls. For auxotrophic selection of diploid cells harbouring prey and bait vectors cells were grown on restrictive growth media lacking tryptophan (-Trp) and Leucine (-Leu). To test specific interaction Adenine (-Ade) was also omitted. (C) Protein-protein interaction screen of the non functional Hfq variants described in Fig. 1 with wild-type Hfq and the C-terminal PilB1 domains as above.

Fig. 3. Complementation of Δ*hfq* with C- and N-terminal eYFP fusion proteins and its localization. Cultures were grown in copper depleted medium to induce protein expression. (A) Altered transcript accumulation of SyR14 as seen in the Δ*hfq* strain is only restored to wild-type levels by Hfq-eYFP. (B) Phototaxis assay showing that only Hfq-eYFP complements the motility phenotype. (C) Subcellular localization of the fusion proteins (Hfq-eYFP, C-terminal fusion; eYFP-Hfq, N-terminal fusion).

Fluorescence images from cells grown on agar plates. eYFP fluorescence is shown in green and chlorophyll fluorescence in magenta.

Fig. 4. Localization of non functional Hfq variants. Fluorescence images showing the alteration in subcellular localization of Hfq variants with a C-terminal eYFP fusion compared to the wild type Hfq-eYFP fusion protein. Cells were grown on agar plates without copper to induce gene expression. eYFP fluorescence is shown in green and chlorophyll fluorescence in magenta. In the wild type Hfq-eYFP strain we observed bright and also multiple weaker spots (mean spots per cell = 3.69 ± 2.44 (SD, n = 78)). In contrast, in mutant P9T, predominantly only one bright spot per cell was visible (mean spots per cell = 1.06 ± 0.33 (SD, n = 71)). Mutants I18F and D42N showed some bright spots as well as intense dispersed eYFP fluorescence in the cytoplasm.

Fig. 5. Significance of PilB1-Hfq interaction for Hfq function and localization. (A) Fluorescence images showing different Hfq-eYFP distribution in the Δ*pilB1* background. eYFP fluorescence is shown in green and chlorophyll fluorescence in magenta. The differences in mean number of spots/cell (Δ*hfq* x Hfq-eYFP = 3.3 ± 2.1 (SD, n = 110 cells)); Δ*pilB1*/Δ*hfq* x Hfq-eYFP = 0.85 ± 0.69 (SD, n = 86 cells)) and mean spot intensity (Δ*hfq* x Hfq-eYFP = 51 ± 41 (a.u.) (SD, n = 166 spots)); Δ*pilB1*/Δ*hfq* x Hfq-eYFP > 240 ± 180 (a.u.) (SD, n = 35 spots)) are statistically significant (Student's *t*-test, $p < 10^{-10}$ in both cases). For the Δ*pilB1* background, mean spot intensity is a minimum estimate because many spots were at saturating intensity with the settings used. (B) Altered transcript accumulation of SyR14 is

evident in Δ*hfq* as well as in all Δ*pilB1* and Δ*pilC* strains. (C) Phototaxis assay of analyzed mutants.

Fig. 6. Simultaneous visualisation of PilB1-sfGFP and Hfq-eYFP in *Synechocystis* cells. A Δ*pilB1* mutant complemented with a sfGFP tagged version of *pilB1* (Fig. S8A) was transformed with the pVZ-*hfq*-eYFP plasmid and grown under inducing conditions. See Experimental Procedures for settings and Supplementary Fig. S8B for controls. sfGFP fluorescence (PilB1) is shown in magenta and eYFP fluorescence (Hfq) in green. Scale-bars 5 microns.

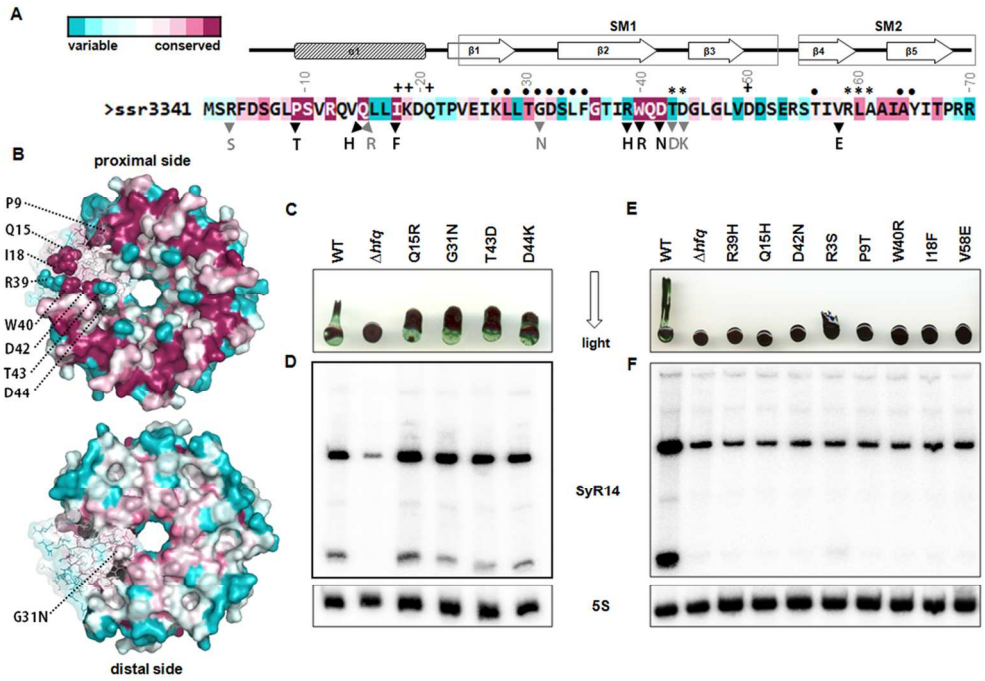

Figure 1
114x77mm (300 x 300 DPI)

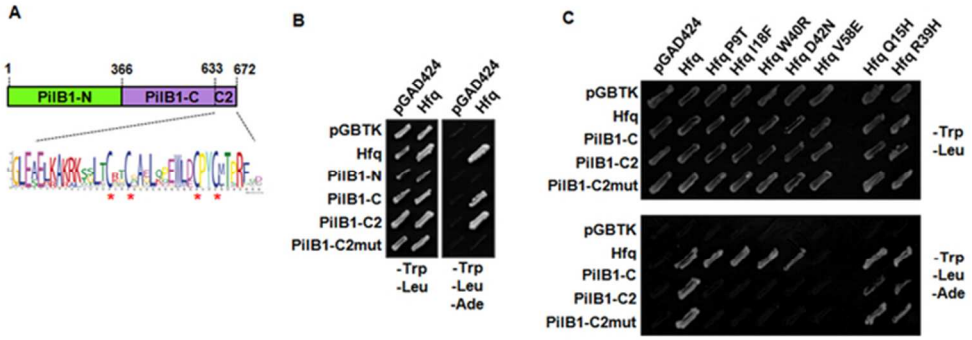

Figure 2
59x20mm (300 x 300 DPI)

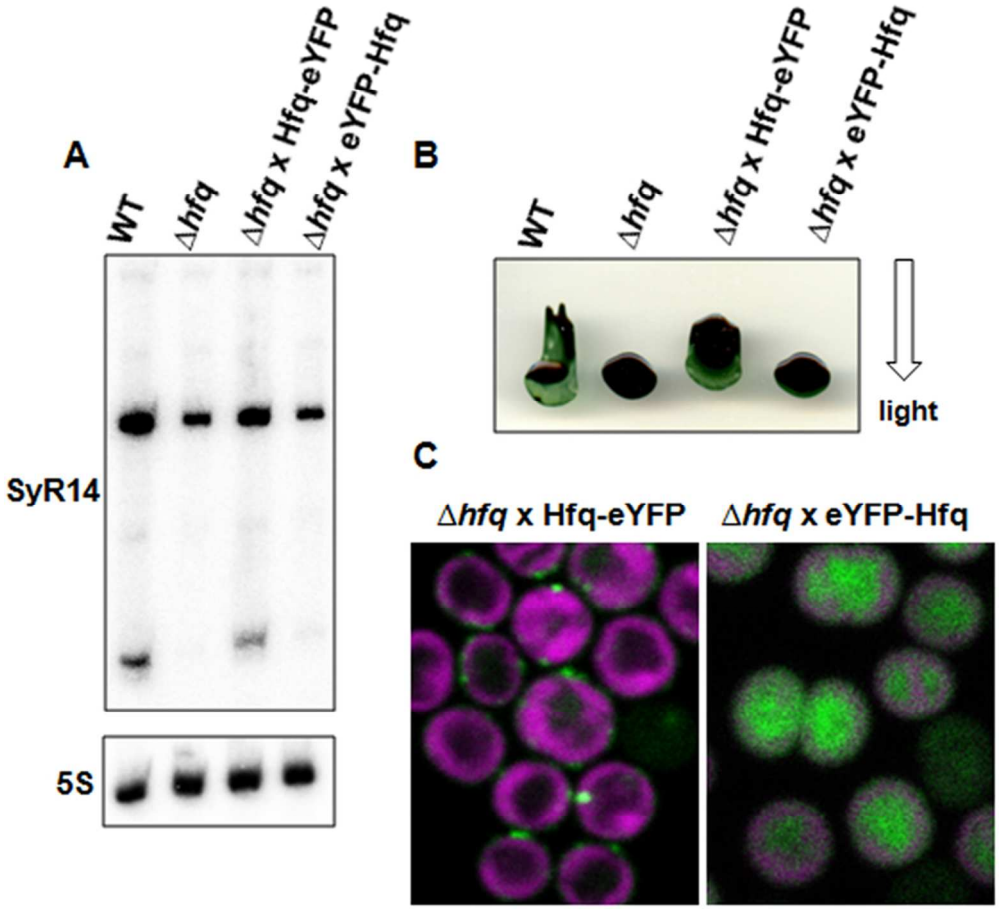

74x69mm (300 x 300 DPI)

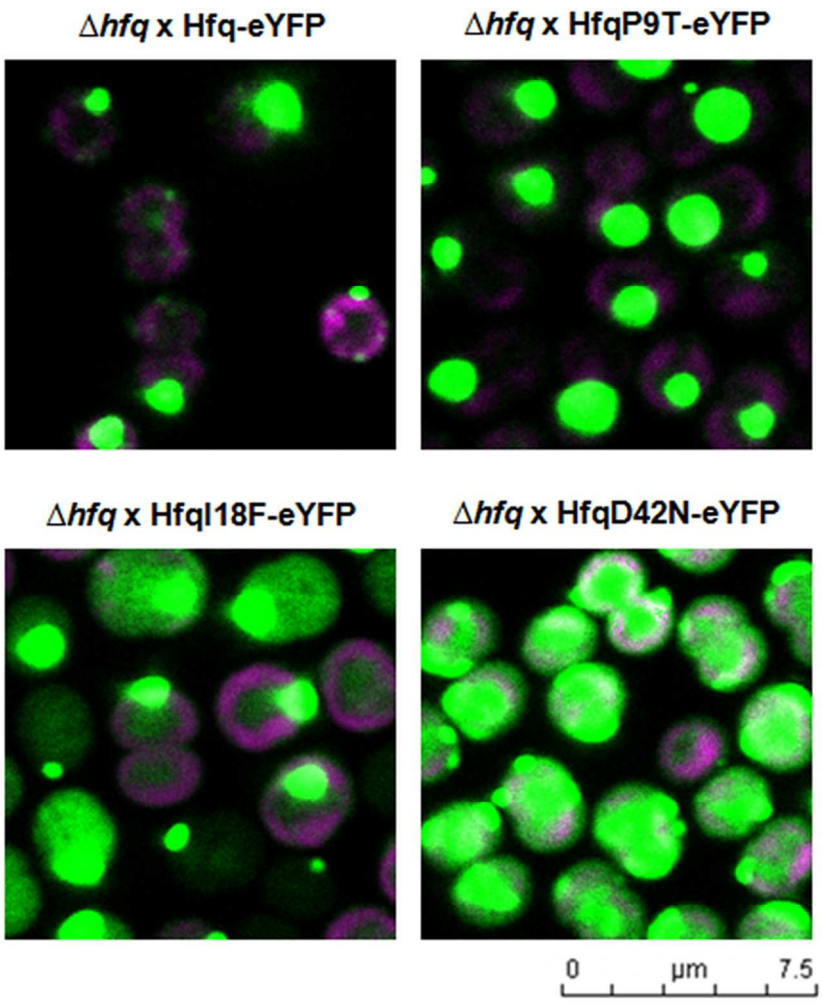

82x84mm (300 x 300 DPI)

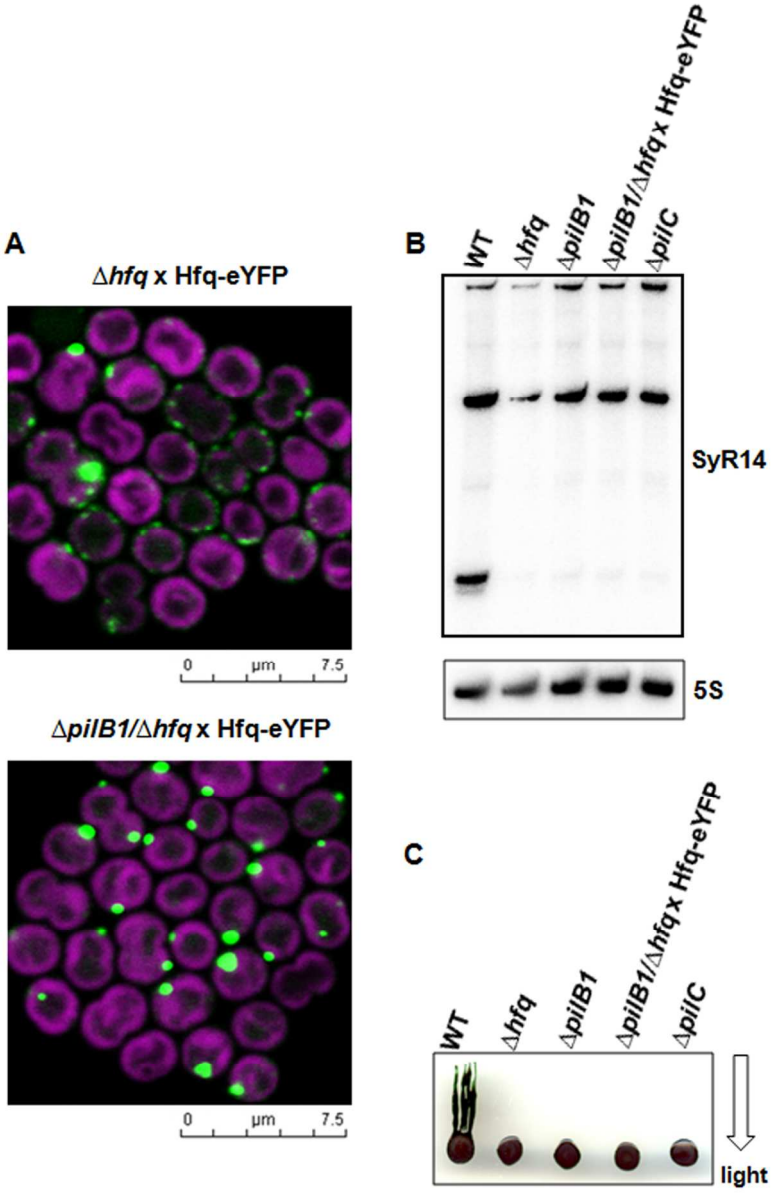

Figure 5
120x182mm (300 x 300 DPI)

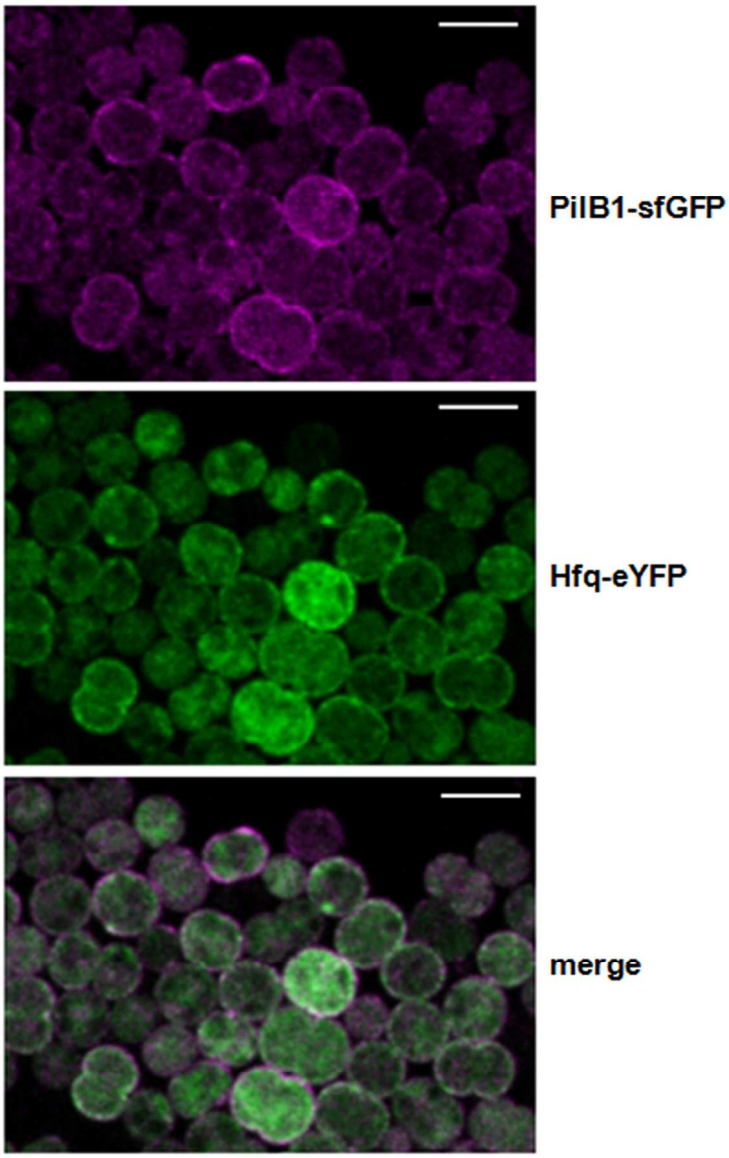

Figure 6
99x124mm (300 x 300 DPI)